Original Article

Title:

Effects of iguratimod on glucocorticoid-induced disorder of bone metabolism in vitro

Authors:

Akira Miyama[a], Kosuke Ebina[b*], Makoto Hirao[a], Gensuke Okamura[c], Yuki Etani[a], Kenji Takami[a], Atsushi Goshima[a], Taihei Miura[a], Shohei Oyama[b], Takashi Kanamoto[d], Hideki Yoshikawa[e], and Ken Nakata[d]

Affiliations:

[a]Department of Orthopaedic Surgery, Osaka University Graduate School of Medicine, 2-2 Yamada-oka, Suita, Osaka 565-0871, Japan

[b]Department of Musculoskeletal Regenerative Medicine, Osaka University Graduate School of Medicine, 2-2 Yamada-oka, Suita, Osaka 565-0871, Japan

[c]Department of Orthopaedic Surgery, Osaka Rosai Hospital, 1179-3 Nagasone-cho, Kita-ku, Sakai 591-8025, Japan

[d]Department of Health and Sport Sciences, Osaka University Graduate School of Medicine, 2-2

Yamada-oka, Suita, Osaka 565-0871, Japan

[e]Department of Orthopaedic Surgery, Toyonaka Municipal Hospital, 4-14-1 Shibaharacho, Toyonaka, Osaka 560-8565, Japan

*_Corresponding author:_

Kosuke Ebina, MD, PhD.

Department of Musculoskeletal Regenerative Medicine, Osaka University Graduate School of Medicine, 2-2 Yamada-oka, Suita, Osaka 565-0871, Japan

Phone: +81-6-6879-3552; Fax: +81-6-6879-3559 E-mail: k-ebina@umin.ac.jp

This article contains 4 figures, 1 table, and 1 Supplementary figure.

Abstract

Glucocorticoids are widely used to treat various diseases including rheumatoid arthritis (RA); however, one of the most frequent and severe adverse effects is glucocorticoid-induced osteoporosis (GIOP). Iguratimod (IGU) is a novel conventional synthetic disease-modifying anti-rheumatic drug developed in Japan. The aim of this study is to investigate the effects of IGU on glucocorticoid-induced disorder of bone metabolism in vitro. IGU significantly suppressed a dexamethasone-induced increase in mouse bone marrow-derived osteoclasts, differentiation, and bone resorption activity by inhibition of the receptor activator of the nuclear factor kappa-B (RANK) /tumor necrosis factor receptor (TNFR)-associated factor 6 (TRAF6)/nuclear factor kappa-B (NFκB)-p52 pathway evaluated by tartrate-resistant acid phosphatase staining, resorption pit assay, western blotting, real-time polymerase chain reaction (PCR), and mRNA sequencing. Concerning osteoblastogenesis of MC3T3-E1 cells, IGU significantly upregulated dexamethasone-induced downregulation of alkaline phosphatase (ALP) activity, bone mineralization, and osteoblast-related protein and gene expression evaluated by ALP staining, alizarin red staining, western blotting, real-time PCR, and mRNA sequencing. In murine osteocyte-like cell line MLO-Y4 cells, IGU significantly upregulated dexamethasone-induced downregulation of the gene expression of ALP and osteocalcin, and also downregulated receptor activator of NFκB ligand (RANKL)/osteoprotegerin gene expression ratio without dexamethasone. Collectively, these results suggest that IGU may

improve glucocorticoid-induced disorder of bone metabolism and may exhibit positive effects against GIOP associated with RA.

Keywords:

glucocorticoid-induced osteoporosis, iguratimod, osteoblast, osteoclast, osteocyte

Introduction

Glucocorticoids are widely used to treat various autoimmune diseases such as rheumatoid arthritis (RA); however, one of the most frequent and severe adverse effects is glucocorticoid-induced osteoporosis (GIOP) [1]. GIOP is associated with increased bone resorption by inducing osteoclastogenesis and decreased bone formation by suppressing osteoblastogenesis, which results in rapid bone loss and increased fracture risk [2,3]. Regarding the treatment of GIOP, the 2017 updated American College of Rheumatology guideline recommended oral bisphosphonates as the first-line agent for patients at moderate or high risk of fracture [4]. However, concerns have arisen about their accumulation within the bone due to high mineral-binding affinities [5], which may lead to adverse effects such as osteonecrosis of the jaw or atypical femoral fracture.

In contrast, according to the European League Against Rheumatism recommendations, primary treatment with conventional synthetic disease-modifying anti-rheumatic drugs (csDMARDs) including methotrexate (MTX) in combination with short-term, low-dose glucocorticoids is

recommended for patients with RA. However, in patients who experienced a treatment failure with MTX alone or who have a contraindication to MTX, other csDMARDs can be used as an additional or substitute treatment, although no reliable criteria exist for their selection, especially in combination with glucocorticoids [6].

Iguratimod (IGU), also known as T-614, is a novel csDMARD developed in Japan. IGU inhibits the production of pro-inflammatory cytokines by macrophages [7] and reduces immunoglobulin production by human B lymphocytes [8] via inhibition of nuclear factor kappa-B (NFκB). In addition, IGU possesses several unique properties concerning bone metabolism that differ from other csDMARDs. We previously reported that IGU promoted bone morphogenetic protein-2 induced bone formation in vivo [9]. In addition, other studies demonstrated that IGU suppressed osteoclast differentiation in RAW264.7 cells [10] and prevented bone loss in ovariectomized mice [11]. However, no studies to date have demonstrated the effects of IGU on GIOP or osteocytes, which remain unclear. The purpose of this study was to investigate the effects of IGU on glucocorticoid-induced disorder of bone metabolism in vitro and to examine the new evidence for the selection of csDMARDs in patients with RA associated with GIOP.

Material and Methods

Ethics statement

Prior to the study, all experimental protocols were approved by the Ethics Review Committee for Animal Experimentation of Osaka University School of Medicine.

Reagents and cell culture

IGU was kindly provided by Toyama Chemical Co. Ltd (Tokyo, Japan), and dissolved in dimethyl sulfoxide (DMSO) (Wako Pure Chemical Industries, Osaka, Japan). Dexamethasone (Dex) was purchased from Sigma-Aldrich (St. Louis, MO, USA) and dissolved in ethanol (Wako Pure Chemical Industries). Murine primary osteoclasts were obtained from bone marrow (BM) cells flushed from the femurs and tibiae of 7-week old male C57BL/6J mice (Charles River Laboratories). These cells were cultured in α-minimum essential medium (α-MEM) (Nacalai Tesque, Kyoto, Japan) containing 10% fetal bovine serum (FBS) (Equitech-Bio, Kerrville, TX, USA) and 1% antibiotic/antimycotic solution (A/A) (Sigma-Aldrich) with 5 ng/mL macrophage colony-stimulating factor (M-CSF) (R&D Systems, Minneapolis, Minnesota, USA) overnight at 37 °C in a humidified atmosphere of 5% carbon dioxide. as previously described [12]. Adherent cells were seeded at 2.4×10^5 cells per well in 12-well or 2×10^4 cells per well in 96-well plates. After 24 hours, osteoclast differentiation was induced with 10 ng/mL M-CSF and 50 ng/mL receptor activator of NFκB ligand (RANKL) (R&D Systems) simultaneously at different concentrations of Dex and/or IGU for 5 days. The concentrations of Dex and IGU were determined based on previous reports [13]. Approximately, the serum concentration of

IGU reaches 3 ug/mL in human.

The MC3T3-E1 cells of osteoblastic cell linage were purchased from Riken Cell Bank (Tsukuba, Japan). The cells were cultured with α-MEM containing 10% FBS in 12-well and 24-well plates at 1×10^5 cells per well. After 24 hours, the cells were treated at different concentrations of Dex and/or IGU in media containing 10 mM β-glycerophosphate (Calbiochem, San Diego, CA, USA) and 50 μg/mL ascorbic acid (Sigma-Aldrich) to induce osteoblast differentiation for 4 days [14].

Murine osteocyte-like cell line MLO-Y4 cells were purchased from Kerafast (Boston, MA, USA) and cultured on type I collagen-coated dishes (Corning, Corning, NY, USA) in α-MEM supplemented with 5% heat-inactivated FBS (Hyclone, Logan, UT, USA), 5% calf serum (Hyclone) and 1% A/A as previously described [15]. The cells were seeded in 24-well plate at 1×10^4 cells per well. After 24 hours, the cells were treated at different concentrations of Dex and/or IGU for 3days.

Tartrate-resistant acid phosphatase staining and resorption pit assay

Tartrate-resistant acid phosphatase (TRAP) staining was performed using a TRAP staining kit (Cosmo Bio, Tokyo, Japan). The total number of TRAP-positive cells with ≥3 nuclei was counted as previously described [12]. Resorption pit assay was performed using Osteo-Assay Surface 96 Well Multiple Well Plates (Corning). Individual pits, or multiple pit clusters, were assayed as previously described [12].

Extraction of the RNA, first-strand complementary DNA synthesis, and quantitative real-time PCR analysis

Total RNA was extracted from cells in a 12-well plate using RNAeasy Mini Kit (Qiagen, Düsseldorf, Germany). First-strand complementary DNA was reverse-transcribed from total RNA (1 μg) using ReverTra Ace quantitative polymerase chain reaction (qPCR) RT kit (Toyobo Co., Ltd., Osaka, Japan) according to the manufacturer's protocol. Real-time PCR (RT-PCR) was performed using a Step One Plus Real-Time PCR System (Life Technologies) and Fast SYBR Green Master Mix (Life Technologies). Gene expression levels were normalized to HPRT1. The sequences of PCR primers are described in **Table 1**.

RNA sequencing and KEGG pathway analysis

After total RNA was extracted, an mRNA sequencing analysis was performed at BGI Tech Solutions Co., Ltd. (Hong Kong) using the DNBseq platform. The differentially expressed genes (DEGs) between the groups were detected with DEseq2 by BGI Tech Solutions, as described [16]. The *p* value cut-off was set at 0.05. A fold change ≥2.00 or ≤0.50 and Q value ≤0.05 were defined to indicate significance. Kyoto Encyclopedia of Genes and Genomes (KEGG) pathway analysis was performed [17], and the most enriched signaling pathways were identified.

145

146 *Western blotting*

147 Western blotting was conducted as previously described [12]. The primary antibodies were as follow:
148 Anti-RANK antibody (1:1000), anti-NFκB p52 antibody (1:1000), anti-Runx2 antibody (1:1000),
149 phosphate anti-extracellular signal-regulated kinase 1/2 (ERK1/2) antibody (Thr202/Tyr204) (1:2000),
150 anti-ERK1/2 antibody (p44/42) (1:1000), phosphate anti-p38 antibody (Thr180/Tyr182) (1:1000),
151 anti-p38 antibody (1:1000), phosphate anti-Stress-activated protein kinase (SAPK)/Jun amino
152 terminal kinase (JNK) antibody (Thr183/Tyr185) (1:1000), anti-SAPK/JNK antibody (1:1000) and
153 β-actin (1:1000) were purchased from Cell Signaling Technology (Danvers, MA, USA). Anti-TRAF6
154 antibody (1:2000), anti-NFATc1 antibody (1:1000), anti-Osterix antibody, anti-Osteocalcin antibody,
155 anti-Sclerostin antibody (1:1000) and anti-DKK1 antibody (1:1000) were purchased from Abcam
156 (Cambridge, MA, USA). Anti-RANKL antibody (1:1000) was purchased from Santa Cruz
157 Biotechnology (Dallas, TX, USA).

158

159 *ALP staining and activity assay*

160 Alkaline phosphatase (ALP) staining was performed by using BCIP/NBT Color Development
161 Substrate (Promega, Madison, WI, USA), and ALP activity was assayed using ALP assay kit (Wako)
162 as previously described [14].

163

164 *Alizarin red staining and bone mineralization quantification*

165 The MC3T3-E1 cells were incubated for 35 days. Alizarin red staining and bone mineralization

166 quantification were performed as previously described [14].

167

168 *Cell proliferation assay*

169 The MC3T3-E1 or MLO-Y4 cells were cultured in 96-well plates at a concentration of 5.0×10^3

170 cells/well. After 24 hours of incubation, the cells were treated with or without Dex and/or IGU. The

171 cell proliferation was assessed every 24 hours using a cell proliferation assay system (Cell Count

172 Reagent SF, Nacalai Tesque) according to the manufacturer's instructions.

173

174 *Statistical analysis*

175 All values were expressed as the mean ± standard deviation. Differences between groups were

176 assessed using the Mann–Whitney U test. Significance was set at $p < 0.05$.

177

178 **Results**

179 *Effects of IGU on Dex-induced promotion of osteoclast number and bone resorption activity in*

180 *mouse BM cells*

The use of Dex significantly promoted RANKL-induced multi-nuclear osteoclast number in a dose-dependent manner, whereas IGU significantly suppressed this phenomenon in a dose-dependent manner within clinical blood concentration (≦3 ug/mL) (**Fig. 1a, 1b**). Both RANKL and Dex significantly promoted resorption activity, whereas IGU significantly inhibited them, regardless of Dex administration (**Fig. 1c, 1d**). Furthermore, an mRNA sequencing assay was performed to examine the possible intracellular signaling pathways. By KEGG pathway analysis, the 10 most enriched pathways were obtained in each group comparison, and osteoclast differentiation signaling (Q = 0.008) and rheumatoid arthritis associated signaling (Q = 0.00009) were one of the significantly enriched pathways compared with or without IGU in the presence of Dex (**Fig. 1e**). These findings suggested that IGU significantly suppressed RANKL and Dex induced osteoclast differentiation and bone resorption activity.

Effects of IGU on Dex-induced upregulation of osteoclastogenesis pathway

By analysis of the KEGG pathway map of osteoclast differentiation, many DEGs were identified, including tumor necrosis factor receptor (TNFR)-associated factor 6 (TRAF6) and its downstream signaling (**Fig. 2a**). Therefore, the study focused on the TRAF6/NFκB/nuclear factor of activated T cells cytoplasmic 1 (NFATc1) signaling pathway and investigated the osteoclast-related genes and proteins expression. In RT-PCR, RANKL significantly increased gene expression of RANK, TRAF6,

NF-κB (p100/p52), RelB, c-Fos, NFATc1, TRAP, DC-STAMP, and cathepsin K. The Dex significantly increased gene expression of RANK and NFATc1. However, IGU significantly suppressed Dex-induced upregulation of RANK, TRAF6, c-Fos, NFATc1, TRAP, DC-STAMP, and Cathepsin K (**Fig. 2b**). Moreover, western blotting was performed to investigate NFκB-p52 at 24 hours because NFκB was activated by RANKL in the early phase of osteoclastogenesis [18]. IGU suppressed protein expression of NFκB-p52 at 24 hours, and RANK, TRAF6, and NFATc1 at 5 days after RANKL stimulation, regardless of Dex administration (**Fig. 2c**). Taken together, IGU suppressed Dex-induced upregulation of osteoclastogenesis via inhibition of RANK/TRAF6/NFκB-p52.

Effects of IGU on Dex-induced downregulation of osteoblast differentiation and bone mineralization in MC3T3-E1 cells

To examine the effects of IGU on Dex-induced osteoblast differentiation and mineralization, ALP and alizarin staining and activity were assayed in MC3T3-E1cells. The IGU significantly promoted ALP activity and bone mineralization, regardless of Dex administration (**Fig. 3 a−d**). In cell proliferation assay, IGU significantly increased cell proliferation without Dex, whereas IGU tended to promote cell proliferation in the presence of Dex (**Fig. 3e**). An mRNA sequencing analysis revealed 3 significantly enriched pathways by IGU (**Fig. 3f**). One of these pathways was the parathyroid hormone (PTH)-activated pathway, and the bglap gene which encoded osteocalcin was differentially expressed

in the KEGG map of PTH-activated pathway as shown in **Supplementary Fig (Online Resource**). By RT-PCR, IGU significantly increased Runx2, osterix, ALP, and osteocalcin regardless of Dex administration (**Fig. 3g**), although the RANKL/OPG expression ratio was not significantly changed. In western blotting, IGU increased protein expression of Runx2 and osterix, regardless of Dex administration (**Fig. 3h**).

Effects of IGU on MLO-Y4 cells in the presence of Dex

Osteocytes are the most abundant source of RANKL to promote osteoclastogenesis, and glucocorticoids induce RANKL and sclerostin expression as well as apoptosis in MLO-Y4 cells [19]. In RT-PCR, Dex significantly decreased the expression of ALP, osteocalcin, and connexin43, whereas IGU significantly increased the gene expression of ALP, osteocalcin, and RANKL/OPG ratio without Dex, and significantly restored the gene expression of ALP, osteocalcin, and connexin43 (**Fig. 4a**). The gene expression of sclerostin coding gene (Sost), dickkopf-1 (Dkk-1), dentin matrix protein 1 (Dmp-1), and fibroblast growth factor 23 (Fgf23) were not significantly changed by IGU. In a cell proliferation assay, Dex significantly decreased cell proliferation, whereas IGU did not affect the results (**Fig. 4b**). In western blotting, IGU promoted the protein expression of osteocalcin, whereas no change was observed in RANKL, sclerostin, and Dkk-1 (**Fig. 4c**). Moreover, the mitogen-activated protein kinases signaling pathway including extracellular signal-regulated kinase (ERK), p-38, and

c-Jun N-terminal kinases (JNK) pathway, which regulated apoptosis or RANKL expression in MLO-Y4 cells, was investigated [20]. The use of IGU promoted phosphorylation of ERK1/2 and p38, especially without Dex, whereas no change was observed in JNK (**Fig. 4d**).

Discussion

To the best of our knowledge, this report is the first to demonstrate the effects of IGU on glucocorticoid-induced disorder of bone metabolism. The study results revealed that IGU significantly suppressed glucocorticoid-induced upregulation of osteoclastogenesis, and significantly restored Dex-induced downregulation of osteoblastogenesis.

Concerning osteoclastogenesis, Dex stimulated RANKL-induced osteoclastogenesis, whereas IGU strongly abolished it. A previous study showed that IGU suppressed osteoclastogenesis via inhibition of PPAR-γ/c-Fos pathway [11]. Indeed, IGU suppressed Dex-induced upregulation of c-fos expression, although the findings of the present study may offer another novel mechanism for this effect. One of the key transcription factors, NF-κB, is activated by RANKL in the early phase [18]. Recent study showed that IGU suppressed nuclear translocation of NFκB-p65 in RAW264.7 cells and RANKL-induced osteoclastogenesis in vitro [21], while our present study demonstrated that IGU inhibited both gene and protein expression of NFκB-p52, which plays an essential role in osteoclastogenesis [18], in mouse bone marrow-derived osteoclasts. This action may lead to inhibition

253 of upstream RANK and TRAF6, which resulted in suppression of osteoclastogenesis [22]. Thus, these
254 results suggest that IGU suppressed glucocorticoid-induced osteoclastogenesis via inhibition of
255 RANK/TRAF6/NFκB-p52.

256 In contrast, glucocorticoids have multiple inhibitory effects on osteoblastogenesis [1]. Consistently,
257 Dex inhibited ALP activity and bone mineralization of MC3T3-E1 cells, whereas IGU significantly
258 restored them in the presence of Dex. These osteogenic effects of IGU may be attributable to
259 upregulation of osteoblast-related gene, such as Runx2 and osterix, as previous reports demonstrated
260 that IGU stimulated osteoblastic differentiation by increased expression of osterix and Dlx5 [9,23].
261 Accordingly, in the present study IGU significantly increased the early osteoblast-related gene and
262 protein expression of Runx2 and osterix, regardless of Dex administration. In addition, the
263 PTH-activated pathway including PTH1 receptor (PTH1R) and osteocalcin expression was
264 significantly enriched by IGU evaluated by RNA sequencing analysis. Specifically, PTH increases the
265 numbers of early osteoblast precursors and hastens their differentiation via PTH1R signaling [24].
266 These results suggest that PTH-activated pathway by IGU may be associated with the significant
267 promotion of cell proliferation and differentiation in MC3T3-E1 cells.

268 Concerning osteocytes, the results of the current study revealed for the first time that IGU
269 significantly increased the gene expression of ALP and osteocalcin in MLO-Y4 cells. A previous
270 study indicated that mature osteocytes strongly expressed mineralization-related genes, such as type I

271 collagen and osteocalcin, compared with young osteocytes in MLO-Y4 cells [25]. Therefore, the
272 current study results suggest that IGU may promote maturation of MLO-Y4 cells. Moreover, IGU
273 significantly inhibited the RANKL/OPG gene expression ratio in MLO-Y4 cells in the current study.
274 Previous studies demonstrated that glucocorticoids increased the RANKL/OPG ratio in osteoblastic
275 cells [26] and RANKL production in MLO-Y4 cells [19]. In contrast, IGU decreased the IL-6-induced
276 elevation of RANKL/OPG ratio in synovial fibroblasts from RA patients [27]. Taken together, IGU
277 may synergistically suppress osteoclastogenesis by inhibition of RANK expression in osteoclasts and
278 also inhibition of RANKL/OPG ratio in osteocytes.
279 Previous studies reported positive effects of csDMARDs and biologic DMARDs on bone
280 metabolisms in vitro [28] [29]. These effects may be partly due to suppression of osteoclastogenesis
281 by interfering with RANKL-mediated induction of NFATc1 or by inhibiting intracellular calcium
282 oscillations depending on Fc receptor gamma. Different from these previous studies, we examined the
283 effects of IGU in osteoclasts, osteoblasts, and osteocytes, concerning glucocorticoid-induced disorder
284 of bone metabolism. However, few studies of csDMARDs and biologic DMARDs showed the
285 significant effects on reducing clinical fractures, while the efficacy of bisphosphonates and
286 denosumab have been established, with reduction of fracture risks [30]. We suppose that this
287 difference may be due to relatively weak inhibitory effects of other csDMARDs or biologic DMARDs
288 on osteoclastogenesis, although bisphosphonates and denosumab exhibit strong inhibitory effect on

289 osteoclastogenesis even under inflammation, glucocorticoids usage, or disuse condition which may
290 promote osteoclastogenesis. Remarkably, our present study demonstrated strong inhibition of
291 osteoclastogenesis by IGU under glucocorticoids usage in vitro.

292 This study has several limitations. First, the study design was in vitro, and further research should be
293 conducted in vivo. Second, a detailed pathway examination using the knock-down and overexpression
294 methods should be considered in the future.

295 In conclusion, IGU significantly suppressed glucocorticoid-induced upregulation of
296 osteoclastogenesis via inhibition of RANK/TRAF6/NFκB-p52. In addition, IGU significantly restored
297 glucocorticoid-induced downregulation of osteoblastogenesis and bone mineralization. These results
298 suggest that IGU may improve glucocorticoid-induced disorder of bone metabolism and that IGU may
299 be considered as one of the preferential treatment options for RA associated with GIOP.

300

301 **Acknowledgment**

302 We would like to thank F. Hirayama and Y. Eguchi for their excellent technical assistance.

303

304 **Conflicts of interest**

305 The iguratimod was kindly provided by Toyama Chemical Co., Ltd (Tokyo, Japan). K. Ebina has
306 received research grants and lecture fee from Eisai. K. Ebina and S. Oyama are affiliated with, and K.

Nakata supervises the Department of Musculoskeletal Regenerative Medicine, Osaka University Graduate School of Medicine, which is supported by Taisho. S. Oyama is an employee of Taisho. These companies had no role in the study design, decision to publish, or preparation of the manuscript.

A. Miyama, M. Hirao, G. Okamura, Y. Etani, K. Takami, A. Goshima, T. Miura, T. Kanamoto, and H. Yoshikawa declare that they have no conflicts of interest.

References

1. Canalis E, Mazziotti G, Giustina A, Bilezikian JP (2007) Glucocorticoid-induced osteoporosis: pathophysiology and therapy. Osteoporos Int 18:1319-28 doi:10.1007/s00198-007-0394-0
2. Naganathan V, Jones G, Nash P, Nicholson G, Eisman J, Sambrook PN (2000) Vertebral fracture risk with long-term corticosteroid therapy: prevalence and relation to age, bone density, and corticosteroid use. Arch Intern Med 160:2917-22 doi:10.1001/archinte.160.19.2917
3. Hansen KE, Kleker B, Safdar N, Bartels CM (2014) A systematic review and meta-analysis of glucocorticoid-induced osteoporosis in children. Semin Arthritis Rheum 44:47-54 doi:10.1016/j.semarthrit.2014.02.002
4. Buckley L, Guyatt G, Fink HA, Cannon M, Grossman J et al. (2017) 2017 American College of Rheumatology Guideline for the Prevention and Treatment of Glucocorticoid-Induced Osteoporosis. Arthritis Rheumatol 69:1521-37 doi:10.1002/art.40137
5. Russell RG, Watts NB, Ebetino FH, Rogers MJ (2008) Mechanisms of action of bisphosphonates: similarities and differences and their potential influence on clinical efficacy. Osteoporos Int 19:733-59 doi:10.1007/s00198-007-0540-8
6. Smolen JS, Landewe R, Bijlsma J, Burmester G, Chatzidionysiou K et al. (2017) EULAR recommendations for the management of rheumatoid arthritis with synthetic and biological disease-modifying antirheumatic drugs: 2016 update. Ann Rheum Dis 76:960-77 doi:10.1136/annrheumdis-2016-210715
7. Du F, Lu LJ, Fu Q, Dai M, Teng JL, Fan W, Chen SL, Ye P, Shen N, Huang XF, Qian J, Bao

CD (2008) T-614, a novel immunomodulator, attenuates joint inflammation and articular damage in collagen-induced arthritis. Arthritis Res Ther 10:R136 doi:10.1186/ar2554

8. Tanaka K, Yamamoto T, Aikawa Y, Kizawa K, Muramoto K, Matsuno H, Muraguchi A (2003) Inhibitory effects of an anti-rheumatic agent T-614 on immunoglobulin production by cultured B cells and rheumatoid synovial tissues engrafted into SCID mice. Rheumatology (Oxford) 42:1365-71 doi:10.1093/rheumatology/keg381

9. Kuriyama K, Higuchi C, Tanaka K, Yoshikawa H, Itoh K (2002) A novel anti-rheumatic drug, T-614, stimulates osteoblastic differentiation in vitro and bone morphogenetic protein-2-induced bone formation in vivo. Biochem Biophys Res Commun 299:903-9 doi:10.1016/s0006-291x(02)02754-7

10. Gan K, Yang L, Xu L, Feng X, Zhang Q, Wang F, Tan W, Zhang M (2016) Iguratimod (T-614) suppresses RANKL-induced osteoclast differentiation and migration in RAW264.7 cells via NF-kappaB and MAPK pathways. Int Immunopharmacol 35:294-300 doi:10.1016/j.intimp.2016.03.038

11. Wu YX, Sun Y, Ye YP, Zhang P, Guo JC, Huang JM, Jing XZ, Xiang W, Yu SY, Guo FJ (2017) Iguratimod prevents ovariectomyinduced bone loss and suppresses osteoclastogenesis via inhibition of peroxisome proliferatoractivated receptorgamma. Mol Med Rep 16:8200-08 doi:10.3892/mmr.2017.7648

12. Noguchi T, Ebina K, Hirao M, Morimoto T, Koizumi K, Kitaguchi K, Matsuoka H, Iwahashi T, Yoshikawa H (2017) Oxygen ultra-fine bubbles water administration prevents bone loss of glucocorticoid-induced osteoporosis in mice by suppressing osteoclast differentiation. Osteoporos Int 28:1063-75 doi:10.1007/s00198-016-3830-1

13. Kohno M, Aikawa Y, Tsubouchi Y, Hashiramoto A, Yamada R, Kawahito Y, Inoue K, Kusaka Y, Kondo M, Sano H (2001) Inhibitory effect of T-614 on tumor necrosis factor-alpha induced cytokine production and nuclear factor-kappaB activation in cultured human synovial cells. J Rheumatol 28:2591-6

14. Kaneshiro S, Ebina K, Shi K, Higuchi C, Hirao M, Okamoto M, Koizumi K, Morimoto T, Yoshikawa H, Hashimoto J (2014) IL-6 negatively regulates osteoblast differentiation through the SHP2/MEK2 and SHP2/Akt2 pathways in vitro. J Bone Miner Metab 32:378-92 doi:10.1007/s00774-013-0514-1

15. Kato Y, Windle JJ, Koop BA, Mundy GR, Bonewald LF (1997) Establishment of an osteocyte-like cell line, MLO-Y4. J Bone Miner Res 12:2014-23 doi:10.1359/jbmr.1997.12.12.2014

16. Love MI, Huber W, Anders S (2014) Moderated estimation of fold change and dispersion for RNA-seq data with DESeq2. Genome Biol 15:550 doi:10.1186/s13059-014-0550-8

17. Kanehisa M, Araki M, Goto S, Hattori M, Hirakawa M, Itoh M, Katayama T, Kawashima

S, Okuda S, Tokimatsu T, Yamanishi Y (2008) KEGG for linking genomes to life and the environment. Nucleic Acids Res 36:D480-4 doi:10.1093/nar/gkm882

18. Franzoso G, Carlson L, Xing L, Poljak L, Shores EW, Brown KD, Leonardi A, Tran T, Boyce BF, Siebenlist U (1997) Requirement for NF-kappaB in osteoclast and B-cell development. Genes Dev 11:3482-96 doi:10.1101/gad.11.24.3482

19. Zhu L, Chen J, Zhang J, Guo C, Fan W, Wang YM, Yan Z (2017) Parathyroid Hormone (PTH) Induces Autophagy to Protect Osteocyte Cell Survival from Dexamethasone Damage. Med Sci Monit 23:4034-40 doi:10.12659/msm.903432

20. Yu C, Huang D, Wang K, Lin B, Liu Y, Liu S, Wu W, Zhang H (2017) Advanced oxidation protein products induce apoptosis, and upregulate sclerostin and RANKL expression, in osteocytic MLO-Y4 cells via JNK/p38 MAPK activation. Mol Med Rep 15:543-50 doi:10.3892/mmr.2016.6047

21. Li CH, Ma ZZ, Jian LL, Wang XY, Sun L, Liu XY, Yao ZQ, Zhao JX (2020) Iguratimod inhibits osteoclastogenesis by modulating the RANKL and TNF-alpha signaling pathways. Int Immunopharmacol 90:107219 doi:10.1016/j.intimp.2020.107219

22. Yamashita T, Yao Z, Li F, Zhang Q, Badell IR, Schwarz EM, Takeshita S, Wagner EF, Noda M, Matsuo K, Xing L, Boyce BF (2007) NF-kappaB p50 and p52 regulate receptor activator of NF-kappaB ligand (RANKL) and tumor necrosis factor-induced osteoclast precursor differentiation by activating c-Fos and NFATc1. J Biol Chem 282:18245-53 doi:10.1074/jbc.M610701200

23. Song J, Liu H, Zhu Q, Miao Y, Wang F, Yang F, Cheng W, Xi Y, Niu X, He D, Chen G (2018) T-614 Promotes Osteoblastic Cell Differentiation by Increasing Dlx5 Expression and Regulating the Activation of p38 and NF-kappaB. Biomed Res Int 2018:4901591 doi:10.1155/2018/4901591

24. Balani DH, Ono N, Kronenberg HM (2017) Parathyroid hormone regulates fates of murine osteoblast precursors in vivo. J Clin Invest 127:3327-38 doi:10.1172/JCI91699

25. Tanaka T, Hoshijima M, Sunaga J, Nishida T, Hashimoto M, Odagaki N, Osumi R, Aadachi T, Kamioka H (2018) Analysis of Ca(2+) response of osteocyte network by three-dimensional time-lapse imaging in living bone. J Bone Miner Metab 36:519-28 doi:10.1007/s00774-017-0868-x

26. Humphrey EL, Williams JH, Davie MW, Marshall MJ (2006) Effects of dissociated glucocorticoids on OPG and RANKL in osteoblastic cells. Bone 38:652-61 doi:10.1016/j.bone.2005.10.004

27. Wei Y, Sun X, Hua M, Tan W, Wang F, Zhang M (2015) Inhibitory Effect of a Novel Antirheumatic Drug T-614 on the IL-6-Induced RANKL/OPG, IL-17, and MMP-3 Expression in Synovial Fibroblasts from Rheumatoid Arthritis Patients. Biomed Res Int

2015:214683 doi:10.1155/2015/214683

28. Suematsu A, Tajiri Y, Nakashima T, Taka J, Ochi S, Oda H, Nakamura K, Tanaka S, Takayanagi H (2007) Scientific basis for the efficacy of combined use of antirheumatic drugs against bone destruction in rheumatoid arthritis. Mod Rheumatol 17:17-23 doi:10.1007/s10165-006-0531-1

29. Okada H, Kajiya H, Omata Y, Matsumoto T, Sato Y et al. (2019) CTLA4-Ig Directly Inhibits Osteoclastogenesis by Interfering With Intracellular Calcium Oscillations in Bone Marrow Macrophages. J Bone Miner Res 34:1744-52 doi:10.1002/jbmr.3754

30. Eastell R, Rosen CJ, Black DM, Cheung AM, Murad MH, Shoback D (2019) Pharmacological Management of Osteoporosis in Postmenopausal Women: An Endocrine Society* Clinical Practice Guideline. J Clin Endocrinol Metab 104:1595-622 doi:10.1210/jc.2019-00221

Figure legends

Fig. 1 IGU significantly suppressed a Dex-induced increase in mouse bone marrow-derived osteoclasts, differentiation, and bone resorption activity. **a** TRAP staining of osteoclasts with M-CSF and RANKL treated at different doses of Dex and/or IGU (×40, scale bar, 500 μm). **b** The number of TRAP-positive cells per well (n = 4 independent experiments' data for each group). **c** TRAP staining and pit formation by osteoclasts (×200, scale bar, 100μm). **d** Quantification of bone resorption area (n = 4 independent experiments' data for each group). **e** KEGG pathway analysis results for the 10 most enriched pathways compared with or without IGU in the presence of Dex. All pathways described were significant (Q < 0.05).

*p < 0.05, **p < 0.01, versus the control group treated with RANKL or treated with RANKL and

Dex.

#$p < 0.05$, ##$p < 0.01$, versus vehicle.

All data are expressed as the mean ± standard deviation.

Dex, dexamethasone; IGU, iguratimod; TRAP, Tartrate-resistant acid phosphatase; RANKL, receptor activator of nuclear factor kappa-B ligand; KEGG, Kyoto Encyclopedia of Genes and Genomes.

Fig. 2 IGU significantly suppressed Dex-induced upregulation of osteoclastogenesis via inhibition of RANK/TRAF6/NFκB-p52. **a** KEGG pathway map of osteoclast differentiation compared with or without IGU in the presence of Dex. Red rectangles represent significantly upregulated, and green rectangles represent significantly downregulated factors. **b** Real-time-PCR analysis of osteoclast-related gene expression at 5 days after RANKL stimulation (n = 5 independent experiments' data for each group). **c** Western blotting analysis of NFκB-p52 at 24 hours, and RANK, TRAF6, and NFATc1 at 5 days after RANKL stimulation.

*$p < 0.05$, **$p < 0.01$, versus control group treated with RANKL or treated with RANKL and Dex.

#$p < 0.05$, ##$p < 0.01$, versus vehicle.

All data are expressed as the mean ± standard deviation.

DC-STAMP, dendritic cell-specific trans-membrane protein; Dex, dexamethasone; HPRT1, hypoxanthine phosphoribosyltransferase 1; IGU, iguratimod; KEGG, Kyoto Encyclopedia of Genes

and Genomes; NFκB, nuclear factor kappa-B; NFATc1, nuclear factor of activated T cells c1; n.s., not significant; RANK, receptor activator of nuclear factor kappa-B; RANKL, receptor activator of nuclear factor kappa-B ligand; TRAF, tumor necrosis factor receptor associated factor; TRAP, tartrate-resistant acid phosphatase.

Fig. 3 IGU significantly restored Dex-induced downregulation of ALP activity, bone mineralization, and osteoblast-related gene and protein in MC3T3-E1 cells. **a** ALP staining, **b** ALP activity, **c** alizarin red staining, and **d** bone mineralization assay (n = 6 independent experiments' data for each group). **e** Cell proliferation assay after 48 hours of treatment with or without Dex and/or IGU (n = 5 independent experiments' data for each group). **f** KEGG pathway analysis results for the 4 most enriched pathways in comparison with or without IGU. **g** Real-time-PCR analysis of osteoblast-related gene expression treated with or without Dex and/or IGU for 4 days (n = 5 independent experiments' data for each group). **h** Western blotting analysis of Runx2 and Osterix treated with or without Dex and/or IGU for 4 days.

*$p < 0.05$, **$p < 0.01$, versus control group treated with vehicle or Dex.

#$p < 0.05$, ##$p < 0.01$, versus vehicle.

All data are expressed as the mean ± standard deviation.

ALP, Alkaline phosphatase; Dex, dexamethasone; IGU, iguratimod; HPRT1, hypoxanthine

phosphoribosyltransferase 1; KEGG, Kyoto Encyclopedia of Genes and Genomes; n.s., not significant; OPG, osteoprotegerin; PCR, polymerase chain reaction; RANKL, receptor activator of nuclear factor kappa-B ligand; Runx2, Runt-related transcription factor 2.

Fig. 4 IGU significantly upregulated Dex-induced downregulation of the gene expression of ALP and osteocalcin, and also downregulated RANKL/OPG gene expression ratio without dexamethasone in murine osteocyte-like cell line MLO-Y4 cells. **a** Real-time-PCR analysis of MLO-Y4 cells for osteocyte-related gene expression treated with or without Dex and/or IGU for 3 days (n = 4 independent experiments' data for each group). **b** Cell proliferation assay after 72 hours of treatment with or without Dex and/or IGU (n = 5 independent experiments' data for each group). **c and d** Western blotting analysis of the osteocyte-related protein expression and the mitogen-activated protein kinases (MAPK) signaling pathway treated with or without Dex and/or IGU for 3 days.

*$p < 0.05$, **$p < 0.01$, versus control group treated with vehicle or Dex.

#$p < 0.05$, ##$p < 0.01$, versus vehicle.

All data are expressed as the mean ± standard deviation.

ALP, alkaline phosphatase; Dex, dexamethasone; Dkk-1, dickkopf-1; Dmp-1, dentin matrix protein 1; ERK, extracellular signal-regulated kinase; Fgf23, fibroblast growth factor 23; HPRT1, hypoxanthine phosphoribosyltransferase 1; IGU, iguratimod; n.s., not significant; OPG, osteoprotegerin; PCR,

polymerase chain reaction; RANKL, receptor activator of nuclear factor kappa-B ligand; SAPK/JNK, stress-activated protein kinase/Jun-amino-terminal kinase; Sost, sclerostin coding gene.

Supplementary Fig. KEGG map of parathyroid hormone activated pathway in comparison with or without IGU in the absence of Dex. Red rectangles represent significantly upregulated factors. Dex, dexamethasone; IGU, iguratimod; PTH, parathyroid hormone; KEGG, Kyoto Encyclopedia of Genes and Genomes.

Table 1 Primers used in RT-PCR

Genes	Forward (5'-3')	Reverse (5'-3')
RANK	AGAAGACGGTGCTGGAGTCT	TAGGAGCAGTGAACCAGTCG
TRAF6	AGCCCACGAAAGCCAGAAGAA	CCCTTATGGATTTGATGATGC
NF-κB (p105/p50)	GAAATTCCTGATCCAGACAAAAAC	ATCACTTCAATGGCCTCTGTGTAG
NF-κB (p100/p52)	CTGGTGGACACATACAGGAAGAC	ATAGGCACTGTCTTCTTTCACCTC
RelA	CTTCCTCAGCCATGGTACCTCT	CAAGTCTTCATCAGCATCAAACTG
RelB	CTTTGCCTATGATCCTTCTGC	GAGTCCAGTGATAGGGGCTCT
c-Fos	AAACCGCATGGAGTGTGTTGTTCC	TCAGACCACCTCGACAATGCATGA
NFATc1	CCGTTGCTTCCAGAAAATAACA	TGTGGGATGTGAACTCGGAA
TRAP	GGGACAATTTCTACTTCACTGGAG	TCAGAGAACACGTCCTCAAAGG
DC-STAMP	GACCTTGGGCACCAGTATTT	CAAAGCAACAGACTCCCAAA
cathepsin K	CCATATGTGGGCCCAGGATG	TCAGGGCTTTCTCGTTCCC
Runx2	GCTTGATGACTCTAAACCTA	AAAAAGGGCCCAGTTCTGAA
osterix	AGGCACAAAGAAGCCATAC	AATGAGTGAGGGAAGGGT
ALP	AATCGGAACAACCTGACTGACC	TCCTTCCACCAGCAAGAAGAA
osteocalcin	CTCACTCTGCTGGCCCTG	CCGTAGATGCGTTTGTAGGC

RANKL	**TGGAAGGCTCATGGTTGGAT**	**CATTGATGGTGAGGTGTGCAA**
OPG	**ACCCAGAAACTGGTCATCAGC**	**CTGCAATACACACACTCATCACT**
Connexin43	**CTCACCTATGTCTCCTCCT**	**CTGGCTTGCTTGTTGTAAT**
Sost	**GGAATGATGCCACAGAGGTCAT**	**CCCGGTTCATGGTCTGGTT**
Dkk-1	**GAGGGGAAATTGAGGAAAGC**	**AGCCTTCTTGTCCTTTGGTG**
Dmp-1	**AGATCCCTCTTCGAGAACTTCGCT**	**TTCTGATGACTCACTGTTCGTGGGTG**
Fgf23	**GATCCCCACCTCAGTTCTCA**	**CCGGATAGGCTCTAGCAGTG**
HPRT1	**CTGGTGAAAAGGACCTCTCGAA**	**CTGAAGTACTCATTATAGTCAAGGGCAT**

receptor activator of nuclear factor kappa-B (RANK) ; tumor necrosis factor receptor associated factor 6 (TRAF6) ; nuclear factor-kappa B (NFκB) ; nuclear factor of activated T cells c1 (NFATc1) ; tartrate resistant acid phosphatase (TRAP) ; dendritic cell-specific trans-membrane protein (DC-STAMP) ; Runt-related transcription factor 2 (Runx2) ; alkaline phosphatase (ALP) ; receptor activator of NF-κB ligand (RANKL) ; osteoprotegerin (OPG) ; dickkopf-1 (Dkk-1) ; dentin matrix protein1 (Dmp1) ; fibroblast growth factor23 (Fgf23) ; hypoxanthine phosphoribosyltransferase 1 (HPRT1)

Figure1

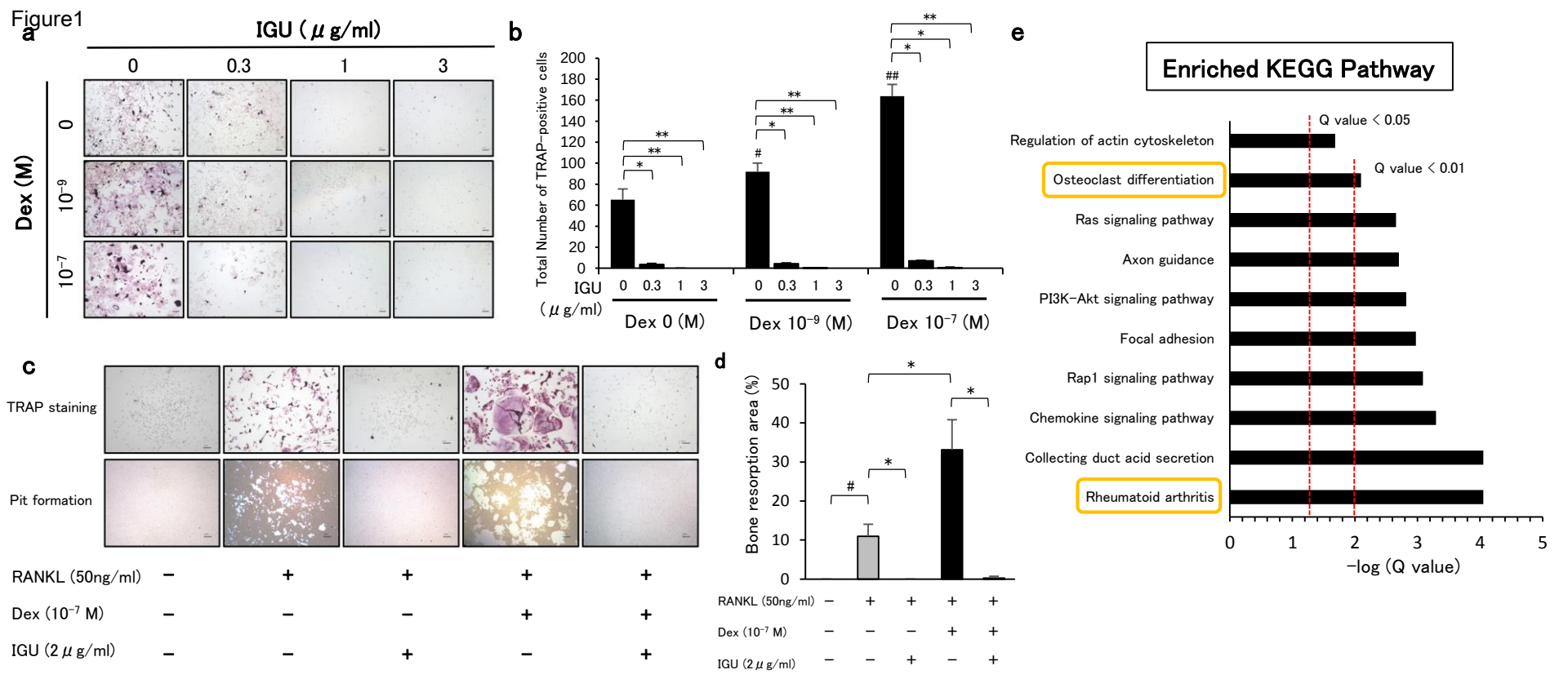
a
IGU (μg/ml)
0
0.3
1
3
Dex (M)
0
10−9
10−7
b
Total Number of TRAP-positive cells
200
180
160
140
120
100
80
60
40
20
0
IGU
0 0.3 1 3
(μg/ml)
Dex 0 (M)
Dex 10−9 (M)
Dex 10−7 (M)
c
TRAP staining
Pit formation
RANKL (50ng/ml) − + + + +
Dex (10−7 M) − − − + +
IGU (2 μg/ml) − − + − +
d
Bone resorption area (%)
50
40
30
20
10
0
RANKL (50ng/ml) − + + + +
Dex (10−7 M) − − − + +
IGU (2 μg/ml) − − + − +
e
Enriched KEGG Pathway
Q value < 0.05
Q value < 0.01
Regulation of actin cytoskeleton
Osteoclast differentiation
Ras signaling pathway
Axon guidance
PI3K-Akt signaling pathway
Focal adhesion
Rap1 signaling pathway
Chemokine signaling pathway
Collecting duct acid secretion
Rheumatoid arthritis
0 1 2 3 4 5
−log (Q value)

Figure2

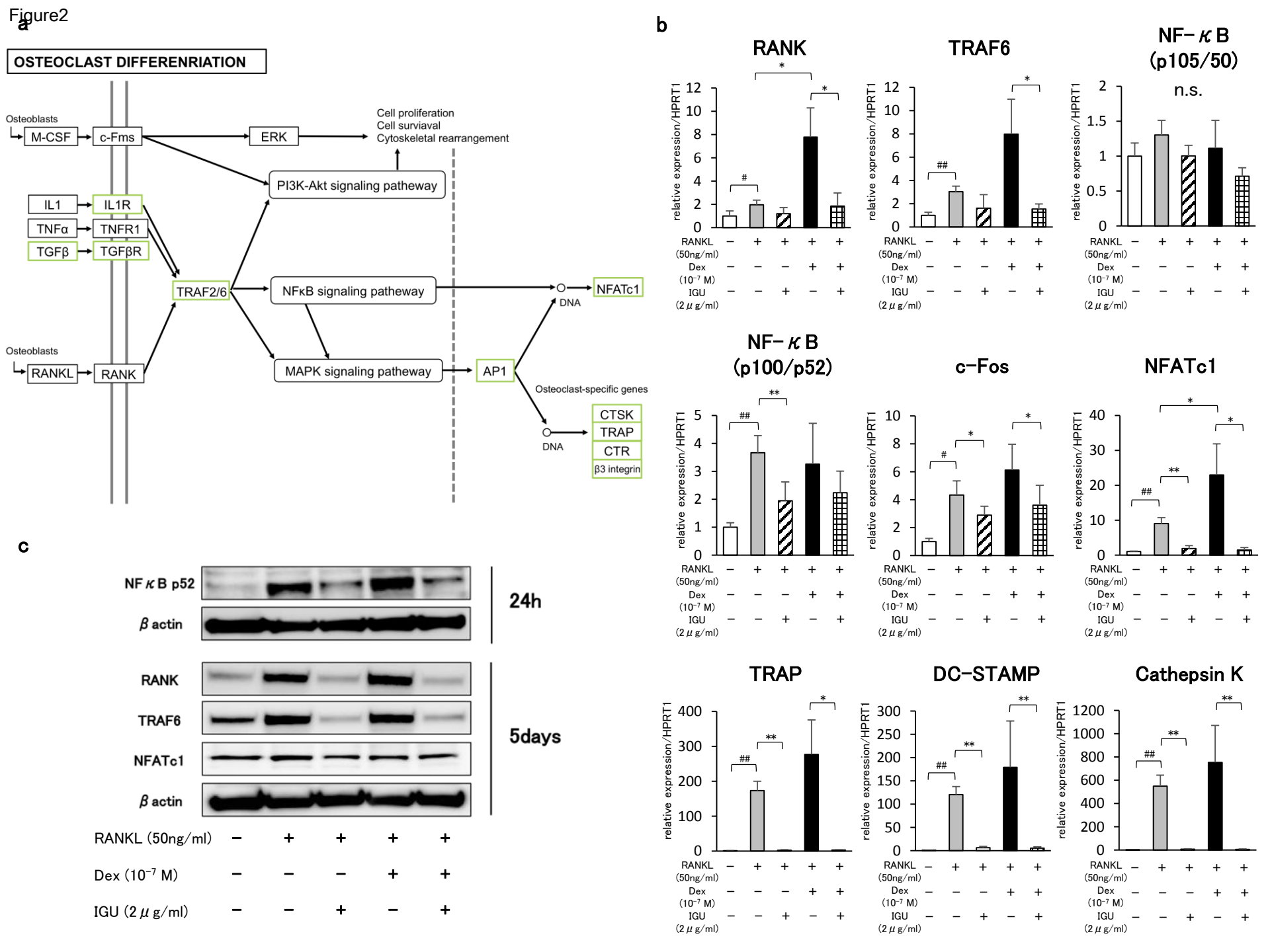
a
OSTEOCLAST DIFFERENRIATION
Osteoblasts
M-CSF
c-Fms
ERK
Cell proliferation
Cell survival
Cytoskeletal rearrangement
PI3K-Akt signaling patheway
IL1
IL1R
TNFα
TNFR1
TGFβ
TGFβR
TRAF2/6
NFκB signaling patheway
NFATc1
DNA
Osteoblasts
RANKL
RANK
MAPK signaling patheway
AP1
Osteoclast-specific genes
DNA
CTSK
TRAP
CTR
β3 integrin
b
RANK
TRAF6
NF-κB (p105/50)
n.s.
NF-κB (p100/p52)
c-Fos
NFATc1
TRAP
DC-STAMP
Cathepsin K
relative expression/HPRT1
RANKL (50ng/ml)
Dex (10⁻⁷ M)
IGU (2 μg/ml)
c
NF κB p52
β actin
24h
RANK
TRAF6
NFATc1
β actin
5days
RANKL (50ng/ml) − + + + +
Dex (10⁻⁷ M) − − − + +
IGU (2 μg/ml) − − + − +

Figure3

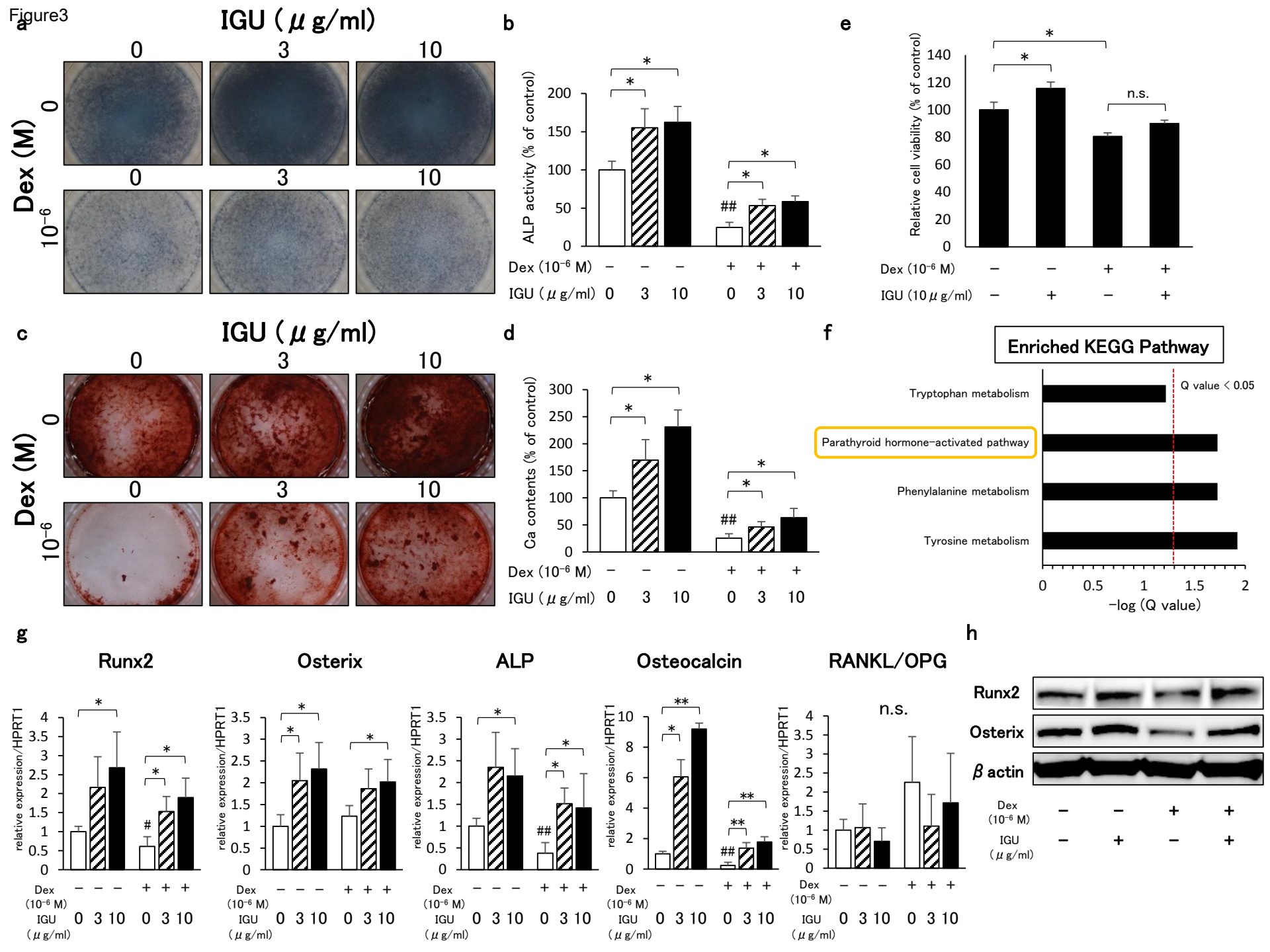
a
IGU (μg/ml)
0
3
10
Dex (M)
0
10⁻⁶
b
ALP activity (% of control)
Dex (10⁻⁶ M)
IGU (μg/ml)
c
Ca contents (% of control)
d
e
Relative cell viability (% of control)
n.s.
IGU (10μg/ml)
f
Enriched KEGG Pathway
Q value < 0.05
Tryptophan metabolism
Parathyroid hormone-activated pathway
Phenylalanine metabolism
Tyrosine metabolism
−log (Q value)
g
Runx2
Osterix
ALP
Osteocalcin
RANKL/OPG
relative expression/HPRT1
h
Runx2
Osterix
β actin

Figure4

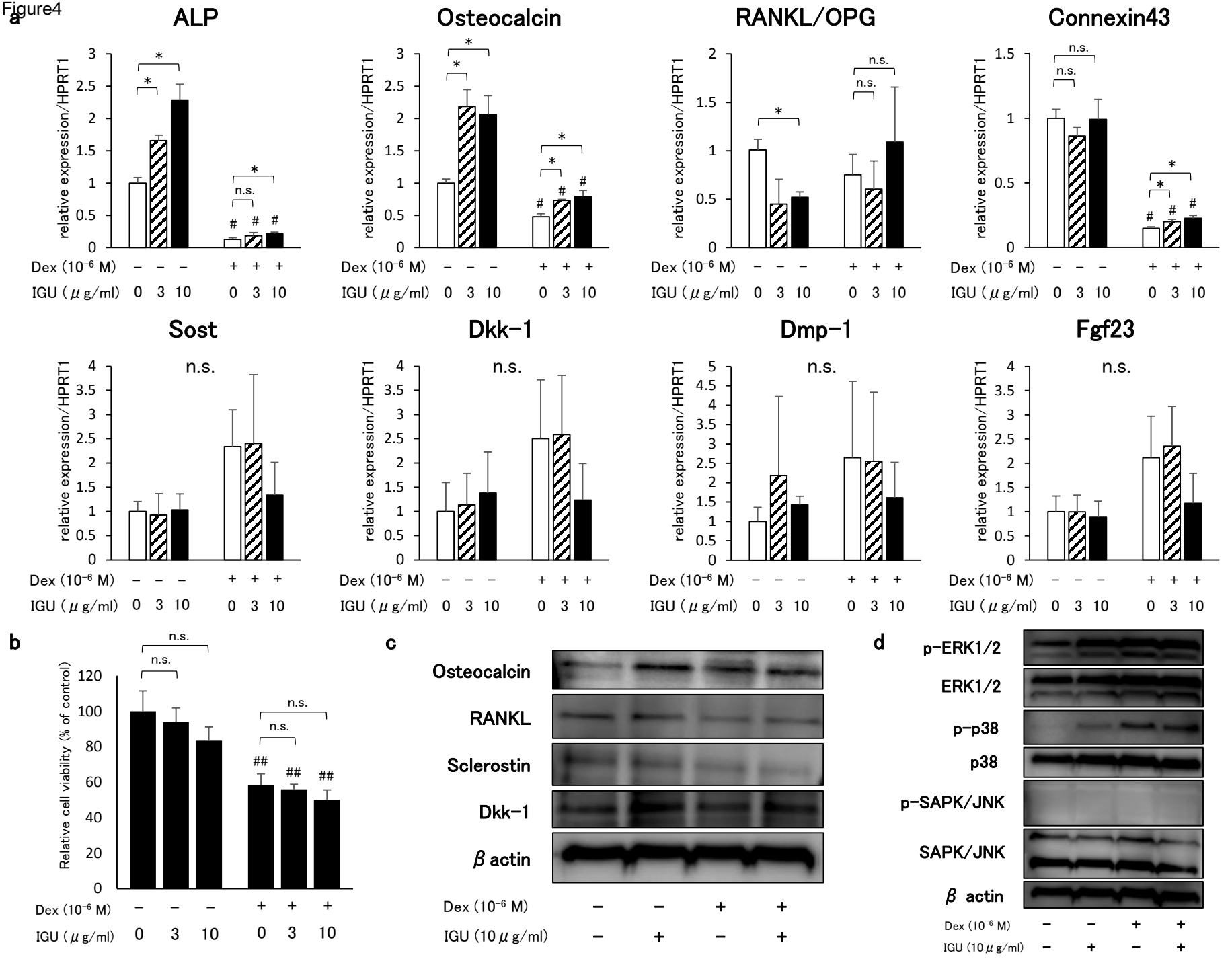
a
ALP
Osteocalcin
RANKL/OPG
Connexin43
Sost
Dkk-1
Dmp-1
Fgf23
relative expression/HPRT1
n.s.
Dex (10⁻⁶ M) – – – + + +
IGU (μg/ml) 0 3 10 0 3 10
b
Relative cell viability (% of control)
c
Osteocalcin
RANKL
Sclerostin
Dkk-1
β actin
Dex (10⁻⁶ M) – – + +
IGU (10 μg/ml) – + – +
d
p-ERK1/2
ERK1/2
p-p38
p38
p-SAPK/JNK
SAPK/JNK
β actin
Dex (10⁻⁶ M) – – + +
IGU (10 μg/ml) – + – +

Supplementary Figure